

RECOVERY OF METALS FROM ELECTROACTIVE COMPONENTS OF SPENT Ni-MH BATTERIES AFTER LEACHING WITH FORMIC ACID

Pedro Rosário Gismonti, Jéssica Frontino Paulino and Júlio Carlos Afonso *

Department of Analytical Chemistry, Institute of Chemistry, Federal University of Rio de Janeiro, Cidade Universitária, Ilha do Fundão, 21941-909, Brazil

Article Info:

Received:
17 August 2020
Revised:
1 February 2021
Accepted:
16 February 2021
Available online:
31 March 2021

Keywords:

Spent Ni-MH batteries
Formic acid
Solvent extraction
Oxalates
Sodium formate

ABSTRACT

This work describes a route for recovering nickel, cobalt, iron, zinc, and lanthanides from spent nickel-metal hydride batteries. Formic acid was used as leachant. Experiments were run at 25-50°C for 1-4 h. Under the best conditions leaching yields surpassed 99 wt.%, except for iron. The insoluble matter contains almost solely iron as iron(III) basic formate. The leachate went through six separation procedures, combining solvent extraction with D2EHPA as extractant, and precipitation reactions. Fe²⁺ and Zn²⁺ were extracted together (> 99 wt.%) from the original leachate (pH ~1.5). Yttrium and lanthanides were precipitated as oxalates directly from the raffinate (> 99.9 wt.%) upon addition of sodium oxalate. In the next steps, Mn²⁺ and Co²⁺ were extracted with D2EHPA at buffered pH (3 and ~4.8, respectively), after adding NaOH_{aq}. About 10 wt.% of leached Ni²⁺ was coextracted with Co²⁺. The remaining Ni²⁺ was precipitated from the raffinate after addition of aqueous sodium oxalate at pH 6. After precipitation of Al³⁺ upon addition of NaOH_{aq} until pH ~8, sodium formate was recovered after slow evaporation of the final aqueous solution at 60°C. It contains ~90 wt.% of the formate present in the leachant.

1. INTRODUCTION

Rechargeable nickel–metal hydride (Ni–MH) batteries are widely used as a power source for small devices such as mobile phones, digital cameras, toys (Fila et al., 2019) and are also found in hybrid electric vehicles (HEV) (Meshram et al., 2017; Korkmaz et al., 2018). Ni–MH batteries have replaced common AA and AAA sizes Zn–C (alkaline and Leclanché) batteries in Brazil (Fernandes et al., 2012, 2013) and nickel–cadmium (Ni–Cd) cells.

The cathode is a porous polymer impregnated with a “paste” containing active nickel compounds and Ni(II) hydroxide. The anode is also composed of a porous polymer impregnated with a mixture of metals including rare earth elements (REEs) and others such as Fe, Co, Ni, Cu, Zn, Al, capable of hydride formation. The active anode is hydrogen ions which during charging and discharging of the battery are absorbed and desorbed by the above mentioned metals. The electrodes are separated by a synthetic porous membrane which enables the contact of electrolyte (KOH solution) contained in electrode space with both electrodes (Fila et al., 2019). The electrode charging and discharging processes are described in the literature (Lucas et al., 2015).

Ni–MH batteries contain base and valuable metals such as REEs, nickel and cobalt in considerable amounts (Oliveira et al., 2017; Meshram et al., 2016). Consumption of REEs, a group of 17 elements including the lanthanides (La–Lu), Sc and Y, has increased significantly in recent years due to their application in high technology areas, including magnets (computers, wind turbines etc.), phosphor powders (fluorescent lamps/tubes), Ni–MH batteries, catalysts, special glasses and metal alloys. Resources of REEs are neither abundant nor evenly distributed across the world (Meshram et al., 2016). REEs have been declared as high supply risk materials by the European Commission (Korkmaz et al., 2018).

The cost and environmental problems associated with the disposal of wastes and scraps in landfills have emerged as the major concern for most nations (Musariri et al., 2019), and also means a waste of non-renewable resources (Gao et al., 2018; Shih et al., 2019; Fu et al., 2019). Recycling of such wastes and scraps may significantly reduce the dependence on primary resources of many elements. Spent Ni–MH batteries are one of such wastes which may be turned to a potential secondary resource (Meshram et al., 2019).

Several hydrometallurgical processes have been

* Corresponding author:
Júlio Carlos Afonso
email: julio@iq.ufrj.br

worked out on different scales to recover metals from spent Ni–MH batteries. Sulfuric and hydrochloric acids have been widely used as leachants (Fernandes et al., 2013; Santos et al., 2014; Turek, 2018; Korkmaz et al., 2018; Oliveira et al., 2017), in the concentration range from 1 to 12 mol L⁻¹, at a temperature range from 25 to 95°C, over a long period of time (> 80 min) (Turek, 2018). The addition of a reductant like hydrogen peroxide improves leaching of many metals as it converts sparingly soluble forms in higher oxidation states (e.g., Co³⁺, Ni³⁺, Mn⁴⁺) to lower valence ions (e.g., Co²⁺, Ni²⁺, Mn²⁺) which are leachable and stable in acidic solution (Vieceli et al., 2018; Santos et al., 2014).

Disposal of acidic leachates is one of the main problems leading to economic and energy losses (Wang et al., 2020; Chen et al., 2018). An opportunity to reduce the environmental impact of hydrometallurgical processes lies in the use of organic acids as leachants. They are biodegradable, delay corrosion of equipments, are safer to handle and emit less toxic gases than strong acids (Gao et al., 2018; Meshram et al., 2020). Studies involving organic acids (citric, oxalic, acetic) only focused the leaching step (Alonso et al., 2017; Colmenares et al., 2018). Separation and purification steps are required for recovery of metal ions from their leachates. It may be difficult to extract many elements due to the strong chelation of some metal ions with carboxylic anions (Fu et al., 2019).

Leached elements are usually separated one from each other by a combination of separation techniques. REEs may either be recovered by solvent extraction (Xie et al., 2014; Paulino et al., 2018) or precipitated as oxalates (Fernandes et al., 2013; Josso et al., 2018; Yang et al., 2014; Oliveira et al., 2017). The use of aqueous two-phase systems (ATPSs) and ion-exchange resins have been also tested for REE recovery (Valadares et al., 2018; Fila et al., 2019). Multiple stages are generally required to separate Co(II) from Ni(II), which have similar chemical properties (Gaines, 2018; Dhiman and Gupta, 2019).

Like oxalic acid, formic acid, the simplest aliphatic monocarboxylic acid, is a strong reductant, but does not precipitate metal ions as does oxalate (Lurie, 1978; Feigl, 1958). It is a versatile renewable reagent for green and sustainable chemical synthesis and processes. It is safer to handle than concentrated inorganic acids (Vieceli et al., 2018; Liu et al., 2015). It is a promising candidate as a leachant for spent batteries (Fu et al., 2019; Ibiapina et al., 2018; Silva et al., 2018), particularly Li-ion ones. Apparently, less attention has been paid to processing of spent Ni–MH batteries in the presence of organic acids. Therefore, the objective of the present investigation is to develop a hydrometallurgical process to recover base metals and REEs from the electroactive components of spent Ni–MH batteries in the presence of formic acid as leachant, while optimizing various parameters such as acid concentration, leaching time and temperature. The novelty elicited in this research is to determine the effectiveness of this acid as a leachant for spent Ni–MH batteries in the place of strong inorganic acids and the feasibility of leachate processing by current separation techniques.

2. MATERIALS AND METHODS

2.1 Samples

120 spent AA Ni–MH batteries (the most common rechargeable size in Brazil) were collected from the local market. To prevent short-circuiting and self-ignition during dismantling, samples were completely discharged first. After manual dismantling, the electroactive components (cathode, anode, electrolyte) were separated. This mass was dried at 105°C for 3 h before being ground using a ball mill and sieved through a 100 µm sieve. In previous work by this research group, elemental analysis was performed by X-ray fluorescence (Fernandes et al., 2013) using the same equipment and procedure described in Section 2.7. Data are presented in Table 1. Water is basically the volatile component lost during drying.

2.2 Reagents

Di-2-ethylhexylphosphoric acid (D2EHPA, 98 wt.%) was supplied by Sigma-Aldrich. n-Hexane (Sigma-Aldrich) was used as diluent. Formic acid (Sigma-Aldrich, 88 wt.%, ~20 mol L⁻¹), sulfuric acid (Merck, 98 wt.%, ~18 mol L⁻¹), sodium hydroxide (6 mol L⁻¹) and sodium oxalate (Merck) were of analytical grade. The solutions were prepared with distilled water.

2.3 Leaching

Baased on leaching studies involving electroactive components of spent batteries (Meshram et al., 2019, 2020; Fernandes et al., 2013; Chen et al., 2018; Yang et al., 2014), the following variables were studied: temperature (25–50 °C), formic acid concentration (5–15 mol L⁻¹) and time (1–4 h). The sample mass to acidic leachant volume ratio was fixed at 100 g L⁻¹.

Experiments were performed in 150 mL glass beakers equipped with a magnetic stirrer. The leaching temperature

TABLE 1: Chemical analyses data of the electroactive components of spent Ni–MH batteries after drying at 105°C for 3 h (Fernandes et al., 2013).

Element	Amount (wt.%)	Relative standard deviation (%)
La	8.9 ± 0.3	3.4
Ce	2.3 ± 0.4	17.4
Pr-Sm	0.7 ± 0.1	14.3
Y	0.3 ± 0.1	33.3
Mn	1.3 ± 0.1	7.7
Fe	2.7 ± 0.1	3.7
Co	3.2 ± 0.6	18.8
Ni	27.2 ± 1.1	4.0
Zn	0.7 ± 0.1	14.3
Na	3.7 ± 0.6	16.2
K	10.4 ± 0.2	1.9
Ca	0.6 ± 0.2	28.6
Al	0.3 ± 0.1	33.3
Loss of volatiles	37.6 ± 1.4	3.7

was controlled by water bath. The aqueous formic acid was added to the beaker and heated to the required temperature at 200 rotations per minute. The instance when the solid was added to the acidic solution was considered as the start of the experiment.

At the end of the experiment the leachate was filtered (under vacuum) through a quantitative filter paper, yielding a green filtrate and a brown residue. This residue was washed with water (3 mL g⁻¹ processed solid), dried at 110°C for 3 h and weighed. It was then placed in a ceramic

crucible and calcined in a furnace (1000°C, 3 h). The roasted mass was cooled down in the furnace and weighed.

All experiments were performed to verify the reproducibility of them. It was found that the error percentage was on the order of ± 3%.

The separation procedure employed was based on precipitation and solvent extraction techniques conducted under increasing pH and evaporation of the final solution to recover the formate ion. Figure 1 presents the general scheme for elements separation from the leachates.

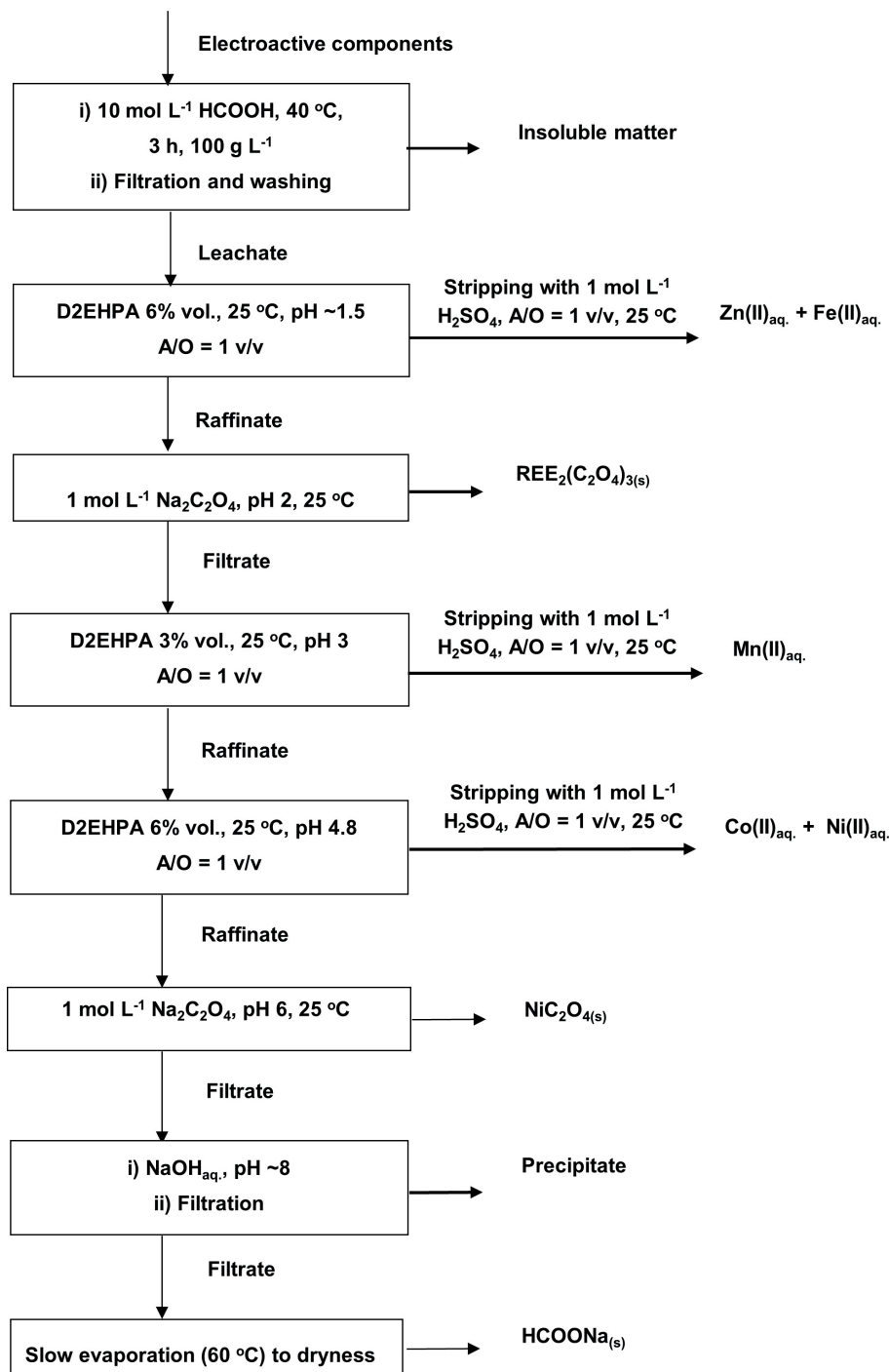


FIGURE 1: General scheme for elements separation from leachates from electroactive components of spent Ni-MH batteries after leaching with HCOOH.

2.4 Solvent extraction of Zn(II), Fe(II), Mn(II) and Co(II) and stripping procedures

Precipitation using hydroxide, sulphide and carbonate does not perform well in a system containing Co(II) and Mn(II) due to their similar chemical properties (Barik et al., 2017). D2EHPA, a cation exchanger, is frequently used as extractant in both research and industrial applications (Virolainen et al., 2011). Extraction experiments were performed in glass separatory funnels at 25°C. Extractant concentration varied from 1 to 10 vol.%. The aqueous/organic (A/O) phase ratio was fixed at 1 vol./vol. pH of the leachate was adjusted by adding the appropriate amount of 6 mol L⁻¹ NaOH. The system was shaken for 5 min. Phase separation was achieved in ~10 min. The experiments were carried out in triplicate and the experimental error including the analytical error was 4% at a confidence level of 95%. The amount of element extracted was calculated by the difference between the concentration in the raffinate and the concentration in the original leachate.

Stripping was carried out at 25°C using aqueous sulfuric acid in glass separatory funnels. Its concentration varied from 0.05 to 5.0 mol L⁻¹. The aqueous/organic (A/O) phase ratio was fixed at 1 vol./vol. The system was shaken for 10 min. Phase separation was achieved in ~5 min. The experiments were carried out in triplicate and the experimental error including the analytical error was 3% at a confidence level of 95%.

2.5 Precipitation of REEs and Ni(II)

Given the high amounts of REEs in the material under study, the method chosen to recover them was the precipitation of their oxalates (Josso et al., 2018; Chiu et al., 2019) at low pH (< 2).

The experiments were accomplished in glass beakers. After solvent extraction of Zn(II) and Fe(II), the raffinate was stirred (200 rotations per minute) at 25°C. 6 mol L⁻¹ NaOH was added dropwise (about 1 mL min⁻¹) in order to adjust pH at ~2. 1 mol L⁻¹ Na₂C₂O₄ was added dropwise until ceased precipitation of a white solid (X₂(C₂O₄)₃, X = Y, La, Ce, Pr, Nd, Sm). It was filtered through a quantitative paper, washed with 0.01 mol L⁻¹ Na₂C₂O₄ and water, dried at 110°C for 3 h and weighed.

After solvent extraction of Co(II), pH of the raffinate was adjusted at ~6 by adding 6 mol L⁻¹ NaOH. 1 mol L⁻¹ Na₂C₂O₄ was added dropwise at 25°C and 200 rpm. A green precipitate (NiC₂O₄) was formed. It was filtered through a quantitative paper and washed with 0.01 mol L⁻¹ Na₂C₂O₄ and water. The filtrate was colorless.

2.6 Crystallization of sodium formate

pH of the raffinate was adjusted to ~8 by adding 6 mol L⁻¹ NaOH at 25°C and 200 rpm. A gelatinous precipitate was formed at pH ~6 (Hayrapetyan et al., 2006) and separated by filtration under vacuum.

The filtrate was slowly evaporated at 60°C (without stirring) in a glass vessel. A white crystalline solid was obtained. It was dried at 110°C for 2 h, ground with an agate mortar and pestle, weighed and kept in a tightly closed container.

2.7 Analytical methods

Metal ion concentrations in the aqueous solutions were determined by atomic absorption spectrometry (AAS) on a Varian/Agilent SpectrAA 50b spectrometer. pH measurements were performed using a combination of a glass electrode and an Ag/AgCl reference electrode (Orion 2Al³-JG). The solids obtained during processing of the leachates were weighed in an analytical balance (Scientech SA 120) and analyzed by X-ray fluorescence (Shimadzu XRF 800 HS). Crystalline phases in the solid samples were identified by X-ray diffraction (Shimadzu XRD 6000) by continuous scanning method at 20 mA and 40 kV, using Cu K α (1.5418 Å) as the radiation source. Data were collected in the two-theta range of 10°-70° (5° min⁻¹).

Classical qualitative tests for Fe(III), Fe(II), Mn(II), Co(II), Zn(II) and Ni(II) were also applied to monitor the presence of such species in the leachates or solids (Vogel, 1981; Feigl, 1958; Lurie, 1978). Detection limits are in the order of 0.1-1.0 mg L⁻¹.

3. RESULTS AND DISCUSSION

3.1 Leaching

3.1.1 Effects of temperature and time

The effects of reaction temperature and time on leaching were investigated using 10 mol L⁻¹ formic acid. The results are shown in Figure 2 and 3 for nickel, lanthanum and iron, the most abundant metals in the electroactive components (Table 1). An increase in the temperature greatly improved leaching of nickel and lanthanum, attaining ~100 wt.% at 40°C after 3 h. A similar effect was observed in some studies involving leaching of Zn-C and Li-ion batteries in the presence of organic acids (Ibiapina et al., 2018; Silva et al., 2018; Musariri et al., 2019). The other REEs behaved as lanthanum. Iron leaching was much less relevant, not surpassing 20 wt.%. Formic acid served the dual role of leachant and reductant for nickel, thus making addition of a reductant like hydrogen peroxide unnecessary.

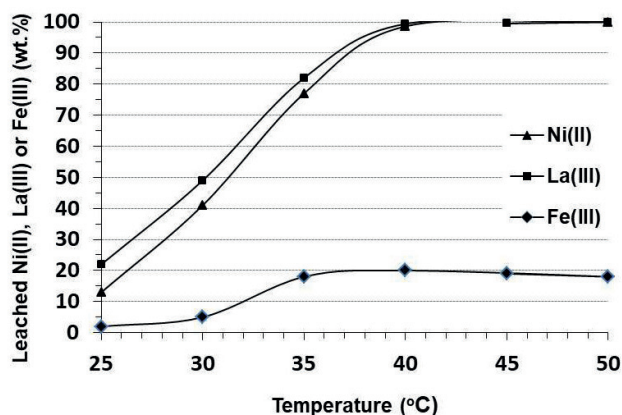


FIGURE 2: Effect of temperature on leaching (10 mol L⁻¹ HCOOH, 3 h, S/L = 100 g L⁻¹).

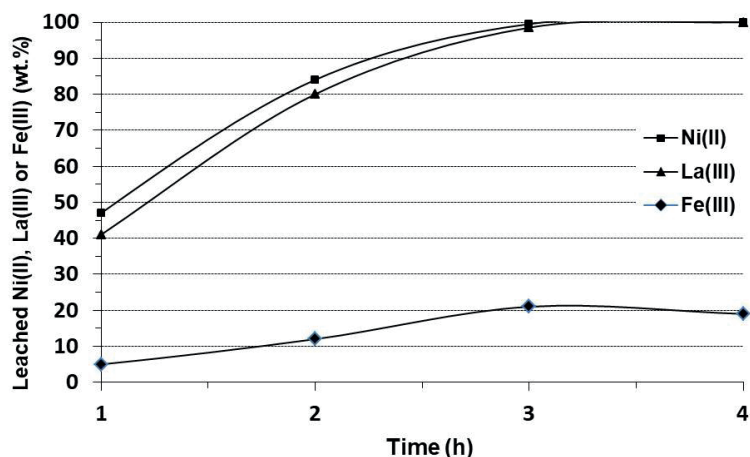


FIGURE 3: Effect of time on leaching (10 mol L⁻¹ HCOOH, 40 °C, S/L = 100 g L⁻¹).

3.1.2 Effect of acid concentration

Figure 4 shows the effect of formic acid concentration on metals leaching under the following conditions: S/L ratio, 100 g L⁻¹; leaching time, 3 h; temperature, 40 °C. When the acid concentration increased from 5 to 10 mol L⁻¹, leaching increased from below 40% to almost 100 wt.%. Thereafter, acid concentrations did not significantly affect the leaching performance. Once again, iron leaching was low in all experiments.

The optimum experimental conditions found for formic acid in the present study are comparable to those normally reported for inorganic acids (Turek, 2018) and for leaching of Li-ion batteries in the presence of organic acids (Fu et al., 2019), except the S/L ratio. In general, literature reports a S/L ratio in the range 2-50 g L⁻¹ (Alonso et al., 2017; Colmenares et al., 2018; Fu et al., 2019; Fernandes et al., 2013; Santos et al., 2014; Korkmaz et al., 2018; Oliveira et al., 2017), but the concentration of the organic acid is much lower (< 5 mol L⁻¹) than in the present study.

3.2 Leachates composition

Table 2 presents the average concentration of elements after leaching under the best experimental conditions (10 mol L⁻¹ HCOOH, 40 °C, 3 h). Based on the chemical analysis presented in Table 1, more than 99 wt.% of all metals present in the electroactive materials were leached under mild conditions with respect to temperature, except iron, where only ~20 wt.% were leached.

3.3 Analysis of the insoluble matter

Under the best conditions (10 mol L⁻¹ HCOOH, 40 °C, 3 h) the brown insoluble matter after leaching corresponds only to 2.2 wt.% of the initial mass. XRF data (Table 3) show that iron is by far the most abundant element, together with minute quantities of nickel and lanthanum. This result agrees with the low iron leaching by formic acid (Table 2). The diffractogram of the insoluble matter is presented in Figure 5. No crystalline phases were identified.

Based on the amount of insoluble matter recovered (2.2 g 100 g⁻¹ electroactive materials), the amounts of iron

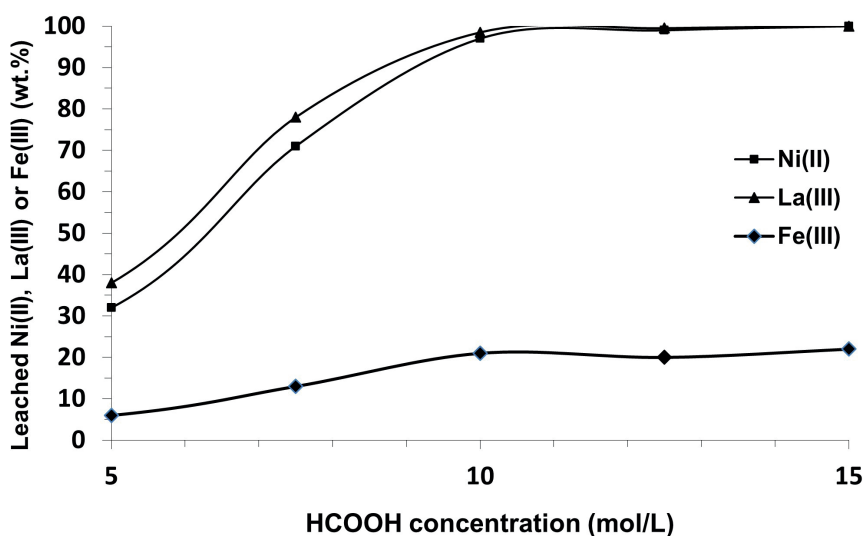


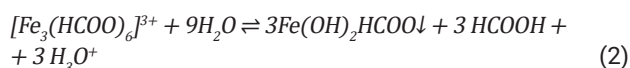
FIGURE 4: Effect of formic acid concentration on leaching (40 °C, 3 h, S/L = 100 g L⁻¹).

TABLE 2: Element concentrations in the leachates.

Element	Concentration (g L ⁻¹)	Relative standard deviation (RSD, %)
Ni	27.7 ± 0.5	1.8
La	8.9 ± 0.4	4.5
Co	3.1 ± 0.3	9.7
Ce	2.3 ± 0.2	8.7
Mn	1.3 ± 0.1	7.7
Pr-Sm	0.7 ± 0.1	14.3
Zn	0.7 ± 0.1	14.3
Ca	0.5 ± 0.1	20.0
Fe	0.5 ± 0.1	20.0
Al	0.3 ± 0.0	0.0
Y	0.2 ± 0.0	0.0
Ca	0.6 ± 0.2	28.6
Al	0.3 ± 0.1	33.3
Loss of volatiles	37.6 ± 1.4	3.7

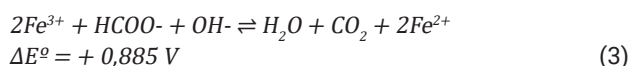
in both solids (Tables 1 and 3) and the leached iron (Table 2), one may conclude that 80 wt.% of iron is present in the insoluble matter. This solid was easily dissolved in 1 mol L⁻¹ H₂SO₄ at 25°C. Only Fe(III) was found in the brown-orange solution formed (Vogel, 1981; Feigl, 1958), the test with thiocyanate in HCl medium was positive.

The ash recovered after calcination of the insoluble matter corresponds to 43 wt.% of the initial mass. It is very likely that the brown solid is iron(III) basic formate (Vogel, 1981):



Fe content in this solid is 41 wt.%, close to the experimental value found.

Soluble iron corresponds to Fe(II), since only the test with α -dipyridyl was positive (Feigl, 1958; Vogel, 1981). This means that formic acid partially reduced Fe(III) (BRATSCH, 1989):



3.4 Solvent extraction of Zn(II), Fe(II), Mn(II) and Co(II)

Zn(II) and Fe(II) were directly extracted from the original leachate (pH ~1.5) using 6 vol.% D2EHPA with high yields (> 99.5 wt.%) in one stage (Figures 6 and 7a). These elements were not detected in the raffinate (Table 4). The tests with dithizone (Zn(II)) and α -dipyridyl (Fe(II)) were negative in the raffinate (Vogel, 1981; Feigl, 1958). The organic phase is pale olive-green (Fe(II)) whereas the raffinate was green (Ni(II)). These results agree with data of Balesini et al. (2011). Stripping of both ions from the loaded organic phase in a single stage was feasible using 1 mol L⁻¹ H₂SO₄ (Figure 8a).

Mn(II) was extracted from pH 2 and was removed from the aqueous phase at pH 3.5 (Figure 6) using 3 vol.% D2E-

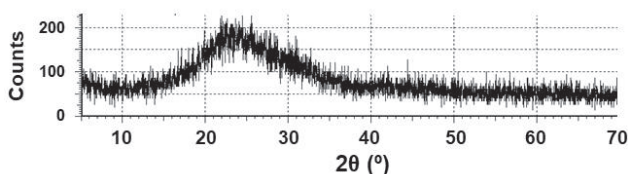
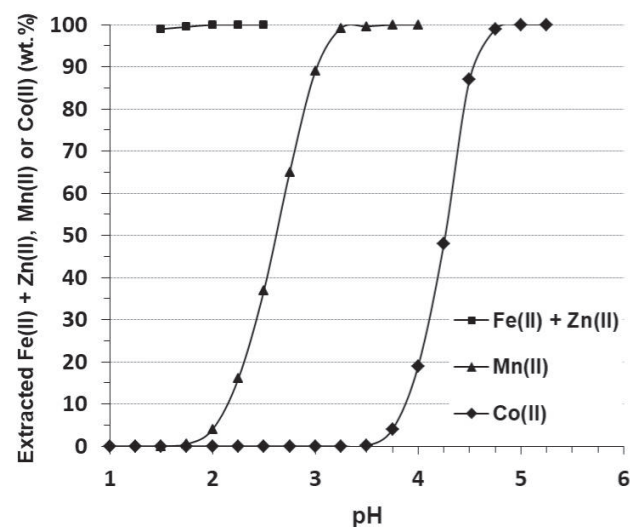
TABLE 3: Chemical analyses data of the insoluble matter after leaching with 10 mol L⁻¹ HCOOH (40°C, 3 h).

Element	Amount (wt.%)
Fe	99.83
Ni	0.15
La	0.02

HPA in one stage. The raffinate contains less than 0.5 wt.% of the element (Table 4). Stripping of Mn(II) from the loaded organic phase in a single stage was feasible using 1 mol L⁻¹ H₂SO₄ (Ibiapina et al., 2018). Since the aqueous phase is colorless, the presence of Mn(II) was monitored using NaBiO₃ + 16 mol L⁻¹ HNO₃ (Vogel, 1981; Feigl, 1958).

Co(II) began to be extracted at pH around 3.8 and was fully extracted at pH ~4.8 (Figure 6). The organic phase was blue due to Co(II). The raffinate was green due to Ni(II). The minimum D2EHPA concentration to ensure Co(II) extraction (> 99.5 wt.%) from the leachate at pH 4.8 in one stage was 6 vol.% (Figure 7b). Under these circumstances, the raffinate contains less than 0.5 wt.% of the element (Table 4). Stripping of Co(II) from the loaded organic phase in a single stage was accomplished using 1 mol L⁻¹ H₂SO₄ (Figure 8b). About 10 wt.% of leached Ni(II) passed to the organic phase. Its concentration in the raffinate (Table 4) is ~10 wt.% lower than in the leachate (Table 2).

The amount of Ni(II) is 8 times higher than Co(II) (Tables 1 and 2). The traditional solvent extraction method

**FIGURE 5:** XDR patterns of the insoluble matter after leaching with 10 mol L⁻¹ HCOOH (40°C, 3 h).**FIGURE 6:** Extraction of Zn(II) + Fe(II), Mn(II) and Co(II) with D2EHPA diluted in kerosene as a function of pH of the leachate. A/O = 1 vol./vol., 25°C, [D2EHPA] = 6 vol.%. Leachant: 10 mol L⁻¹ HCOOH.

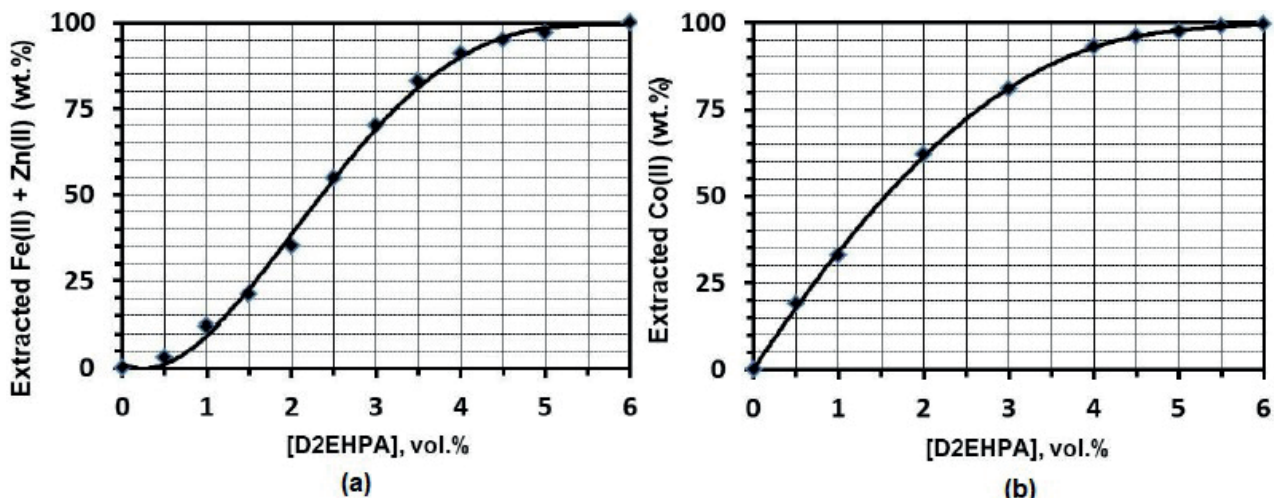


FIGURE 7: Influence of D2EHPA concentration on some elements extraction. A/O = 1 vol./vol., 25°C, pH = 1.5 (Zn(II) + Fe(II)) or 4.5 (Co(II)). Leachant: 10 mol L⁻¹ HCOOH.

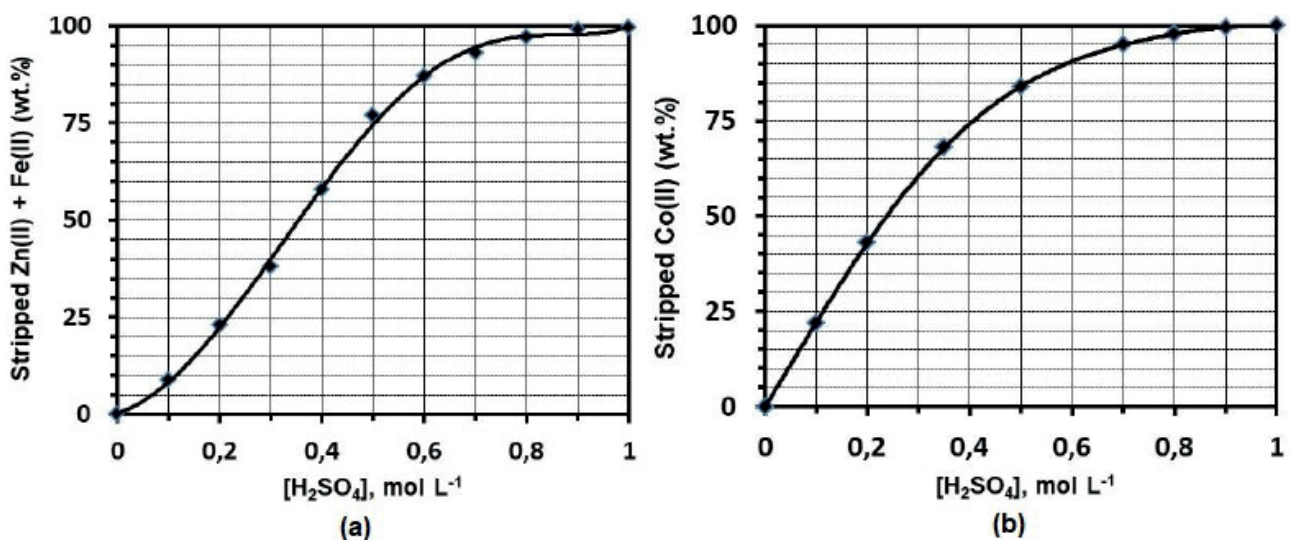


FIGURE 8: Influence of H₂SO₄ concentration on stripping of Zn(II) + Fe(II) and Co(II) from loaded organic phase (A/O = 1 vol./vol., 25°C).

for separating Ni and Co from a leach liquor rich in nickel is prone to cause nickel loss (van der Voorde et al., 2019; Yang et al., 2020). Extraction of Co(II) is more selective at pH below 4, but requires more stages, thus increasing consumption of the extractant and diluent (van der Voorde et al., 2019). Processing of Ni-rich spent materials is feasible by changing the extractant, for example, Cyanex 272 (bis(2,4,4-trimethylpentyl)phosphinic acid) (Janiszewska et al., 2019). It is very selective for cobalt over nickel in sulfate and chloride media (Ayanda et al., 2013).

pH was not practically changed after Mn(II) and Co(II) extractions. Formic acid is a weak acid and its ionization process in aqueous phase can be expressed as follows (Lurie, 1978):



Thus, the leachate was buffered during solvent extraction of Mn(II) and Co(II) by a formic acid/formate buffer (2.77 < pH < 4.77).

The extraction order Zn(II) + Fe(II) – Mn(II) – Co(II) under increasing pH found in this work is the same reported in the literature in sulfate (Ritcey and Ashbrook, 1984) and fluoride media (Silva et al., 2018). This result is in line with the weak ligand character of the formate anion (Lurie, 1978).

Stripping produces a dilute aqueous acidic solution (H₂SO₄) of a metal ion sulfate (ZnSO₄, FeSO₄, MnSO₄, CoSO₄ and NiSO₄) because the metal ion concentrations in the leachate are relatively low (Table 2) and the A/O phase ratio was fixed at 1 v/v. The concentrations in these acidic solutions are very close to the original leachate (Table 2) as both solvent extraction and stripping were performed with high yields (> 99.5 wt.%). Zn(II) can be easily separated from Fe(II) by adding NaOH_{aq} (pH ~11): Fe(OH)₂ precipitates in the presence of soluble [Zn(OH)₄]²⁻. Zn(II) can be recovered as Zn(OH)₂ after neutralizing the alkaline solution with H₂SO_{4aq} (Fernandes et al., 2012). Mn(II) can be precipitated as MnO₂ (or MnO(OH)₂) after adding NaOH_{aq}.

TABLE 4: Element concentrations in the raffinates after solvent extraction and in the aqueous acidic solutions after stripping the loaded organic phase with 1 mol L⁻¹ H₂SO₄

Element	Solvent extraction procedure*	Concentration (g L ⁻¹)	
		Raffinate	Acidic solution
Fe	D2EHPA 6% vol., pH ~1.5	n.d	4.9 x 10 ⁻¹
Zn	D2EHPA 6% vol., pH ~1.5	n.d	7.2 x 10 ⁻¹
Mn	D2EHPA 3% vol., pH ~3	6.0 x 10 ⁻²	1.3
Co	D2EHPA 6% vol., pH ~4.8	1.5 x 10 ⁻²	3.0
Ni	D2EHPA 6% vol., pH ~4.8	2.5 x 10 ¹	2.6

* 25°C, A/O = 1 v/v; n.d. – not detected

(pH ~11) + H₂O₂ (Ibiapina et al., 2018). Co(II) and Ni(II) can also be recovered as hydroxides (Co(OH)₂ and Ni(OH)₂) upon addition of NaOH_{aq}. (pH ~10) (Silva et al., 2018). In all cases an aqueous sodium sulfate is the final product, which can be recovered by slow evaporation of the final solution (Paulino et al., 2018).

3.5 Precipitation of REEs

According to data in Table 5, only small amounts of nickel (~0.1 wt.%) were found. Ni(II) oxalate precipitates at higher pH, usually above 3 (Lurie, 1978; Vogel, 1981; Feigl, 1958).

Based on data in Table 2, 23.4 g of REE oxalates (REE₂(C₂O₄)₃) can be recovered from 1 L of leachate. The experimental value found was 23.3 g L⁻¹. This means that over 99.5 wt.% of lanthanides and yttrium were recovered in this solid. Therefore, precipitation of REE oxalates was a very selective and effective technique under our experimental

TABLE 5: Chemical analyses data of the oxalates (REE₂(C₂O₄)₃ and NiC₂O₄) recovered after processing the leachates (Figure 1) (10 mol L⁻¹ HCOOH, 40 °C, 3 h)

Element	Amount (wt.%)	
	REE ₂ (C ₂ O ₄) ₃	NiC ₂ O ₄
Ni	0.1	98.0
La	73.4	n.d.
Ce	19.2	n.d.
Pr-Sm	5.6	n.d.
Y	1.7	n.d.
Ca	n.d.	2.0

n.d. – not detected

conditions, as the oxalates were recovered with high yield and purity.

An advantage of oxalate salts is their easy conversion to other REE compounds as they are easily thermally decomposed (Yang et al., 2014) and oxidized (Josso et al., 2018).

3.6 Precipitation of Ni(II)

XRF analysis (Table 5) of the green solid found calcium (1.9 wt.%). Based on data in Table 2, 69.2 g of nickel oxalate can be recovered from 1 L of leachate. 63.9 g were recovered, 62.6 g of which correspond to NiC₂O₄ (~90.5 wt.% of the theoretical value). This difference is due to partial solvent extraction of Ni(II) by D2EHPA at pH 4.8 (Section 3.4). 1.3 g of CaC₂O₄ contains ~80 wt.% of leached calcium.

3.7 Crystallization of sodium formate

The solid precipitated at pH ~8 (~0.1 g L⁻¹ processed leachate) contains aluminum and the remaining calcium. According to XRF data (Table 6), the solid also contains minute amounts of nickel (~0.1 wt.%). This step is essential to recover sodium formate with high purity.

The diffractogram (Figure 9) of the white crystalline solid obtained after evaporation of the final aqueous solution corresponds to anhydrous HCOONa. The peaks agree with the standard pattern of monoclinic HCOONa (ICDD PDF Card No. 00-014-0812).

XRF data (Table 6) did not show significant amounts of other metals. However, addition of sodium oxalate to precipitate NiC₂O₄ must be carefully controlled in order to avoid an undesirable excess of oxalate ions, otherwise sodium formate would be contaminated with sodium oxalate.

Sodium formate is a very versatile reactant in laboratory syntheses, in pharmaceutical, textile, paper and leather industries for buffering and regulating of pH (Hietala et al., 2016). This salt is used to produce formic acid. It is a raw material for manufacturing sodium dithionite. Oxalic acid production employs sodium formate as an intermediate. Sodium formate is used in chrome tanning and as a mordant in the dyeing and printing of fabrics by the textile industry. The reducing power of sodium formate is utilized in electroplating baths and photographic fixing baths. (Reutmann and Kieczka, 2012). It is also a food additive (E237) and a deicing agent (Kulyakthin and Paste, 2021).

3.8 Mass balance for formate ion

Based on the composition of the leachant (10 mol L⁻¹ HCOOH), and the mass of the recovered salt, sodium for-

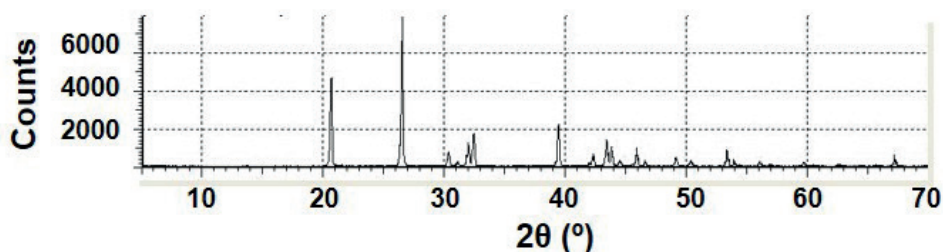


FIGURE 9: XRD patterns of the solid recovered after evaporation of the final solution. The peaks represent HCOONa.

TABLE 6: Chemical analyses data of the solid precipitated at pH ~8 and of sodium formate after evaporation of the final aqueous solution.

Element	Amount (wt.%)	
	Solid	HCOONa
Ni	0.1	n.d.
Ca	25.0	n.d.
Al	74.6	n.d.
Na	0.3	100
REEs	n.d.	n.d.

n.d. – not detected

TABLE 7: Mass balance for formate ion (base: 1 L leachate).

Product/Leachant	Mass (g)	Mass of HCOO ⁻ (g)	Relative amount (wt.%)
10 mol L ⁻¹ HCOOH	-	450.0	100
HCOONa	603.7	399.5	89
Losses	-	50.5	11

mate contains around 90 wt.% of the total formate (Table 7). Two potential sources of loss of formate ions were identified: (i) during leaching, when it acts a reductant; (ii) as iron(III) basic formate. The huge amount of the salt recovered is due to the concentration of formic acid in the leachant (10 mol L⁻¹).

On an average basis, the price of sodium formate (99 wt.%) is about 1.5 times the cost of formic acid (95-98 wt.%) (Hietala et al., 2016; Reutmann & Kieczka, 2012).

4. CONCLUSIONS

Under the best experimental conditions (10 mol L⁻¹ HCOOH, 40°C, 3 h), nickel, manganese, cobalt, zinc and REEs were leached from the electroactive components of spent Ni-MH batteries with very high yields as found for common inorganic acids. The insoluble matter contains ~80 wt.% of the iron present in the original mass as Fe(III) basic formate. The remaining iron was in the leachate as Fe(II).

Recovery of leached elements by solvent extraction using D2EHPA and precipitation of REE and Ni(II) oxalates at suitable pH was possible. The original leachate allowed direct extraction of Zn(II) + Fe(II) and REE oxalates were directly recovered from the raffinate. However, the recovery of Co(II) in the presence of large amounts of Ni(II) by solvent extraction requires further studies. About 90 wt.% of formate present in the leachant was recovered as sodium formate after evaporation of the final solution.

Formic acid has proven a promising leachant for spent Ni-MH batteries: i) it played the dual role of leachant and reductant for nickel, thus avoiding addition of a reductant like hydrogen peroxide; ii) the elements were leached with very high yields (except iron); iii) its leachates were easily processed; iv) a high-value added byproduct was recovered (sodium formate), thus reducing generation of final wastes.

ACKNOWLEDGEMENTS

The authors would like to thank Council of Technological and Scientific Development (CNPq) for financial support. P. R. Gismonti acknowledges PIBIC/CNPq-UFRJ for a fellowship.

REFERENCES

- Almeida, J. R., Moura, M. N., Barrada, R. V., Barbieri, E. M. S., Carneiro, M. T. W. D., Ferreira, S. A. D., Lelis, M. F. F., Freitas, M. B. J. G. & Brandão, G. P., 2019. Composition analysis of the cathode active material of spent Li-ion batteries leached in citric acid solution: A study to monitor and assist recycling processes. *Sci. Total Environ.*, 685, 589–595. <https://doi.org/10.1016/j.scitotenv.2019.05.243>
- Alonso, A.R., Pérez, E.A., Lapidus, G.T. & Luna-Sánchez, R.M., 2017. Hydrometallurgical process for rare earth elements recovery from spent Ni-MH batteries. *Can. Metall. Q.*, 54, 310–317. <https://doi.org/10.1179/1879139515Y.0000000013>
- Ayanda, O. S., Adekola, F. A., Baba, A. A., Ximba, B. J. & Fatoki, O. S., 2013. Application of Cyanex® extractant in Cobalt/Nickel separation process by solvent extraction. *Int. J. Phys. Sci.*, 8, 89-97. <https://doi.org/10.5897/ijps12.135>
- Balesini, A. A., Razavizadeh, H. & Zakeri, A., 2011. Solvent Extraction of Zinc from Acidic Solution Obtained from Cold Purification Filter Cake of Angouran Mine Concentrate Using D2EHPA. *Iran. J. Chem. Chem. Eng.*, 8, 43-47. http://www.ijche.com/article_10282_813d-0dccc4d682c66c2d73e654476a86.pdf
- Barik, S. P., Prabakaran, G. & Kumar, L., 2017. Leaching and separation of Co and Mn from electrode materials of spent lithium-ion batteries using hydrochloric acid: Laboratory and pilot scale study. *J. Cleaner Prod.*, 147, 37-43. <https://doi.org/10.1016/j.jclepro.2017.01.095>
- Bratsch, S. G., 1989. Standard Electrode Potentials and Temperature Coefficients in Water at 298.5 K. *J. Phys. Chem. Ref. Data*, 18, n. 01. <https://doi.org/10.1063/1.555839>
- Chen, X., Guo, C., Ma, H., Li, J., Zhou, T., Cao, L. & Kang, D., 2018. Organic reductants based leaching: A sustainable process for the recovery of valuable metals from spent lithium ion batteries. *Waste Manage.*, 75, 459–468. <https://doi.org/10.1016/j.wasman.2018.01.021>
- Chiu, K. L., Shen, Y. H., Chen, Y. H. & Shih, K. Y., 2019. Recovery of Valuable Metals from Spent Lithium Ion Batteries (LIBs) Using Physical Pretreatment and a Hydrometallurgy Process. *Adv. Mater.*, 8, 12-20. <https://doi.org/10.11648/j.am.20190801.12>
- Colmenares, A. Z., Salaverría, J. D. & Delvasto, P., 2018. Characterization of the chemical compounds obtained after using acetic acid as leaching agent in the hydrometallurgical treatment of spent Ni-MH batteries. *Revista Producción + Limpia*, 13, 19-29. <http://dx.doi.org/10.22507/pml.v13n1a2>
- Dhiman, S. & Gupta, B., 2019. Partition studies on cobalt and recycling of valuable metals from waste Li-ion batteries via solvent extraction and chemical precipitation. *J. Cleaner Prod.*, 225, 820-832. <https://doi.org/10.1016/j.jclepro.2019.04.004>
- Feigl, F., 1958. *Spot Tests in Inorganic Analysis*. Amsterdam: Elsevier.
- Fernandes, A., Afonso, J. C. & Dutra, A. J. B., 2013. Separation of nickel(II), cobalt(II) and lanthanides from spent Ni-MH batteries by hydrochloric acid leaching, solvent extraction and precipitation. *Hydrometallurgy*, 133, 37-43. <http://dx.doi.org/10.1016/j.hydromet.2012.11.017>
- Fernandes, A., Afonso, J. C. & Dutra, A. J. B., 2012. Hydrometallurgical route to recover nickel, cobalt and cadmium from spent Ni-Cd batteries. *J. Power Sources* 220, 286-291. <https://doi.org/10.1016/j.jpowsour.2012.08.011>
- Fila, D., Hubicki, Z. & Kołodyńska, D., 2019. Recovery of metals from waste nickel-metal hydride batteries using multifunctional Diphonix resin. *Adsorption*, 25, 367–382. <https://doi.org/10.1007/s10450-019-00013-9>
- Fu, Y., He, Y., Chen, H., Ye, C., Lu, Q., Li, Xie, W. & Wang, J., 2019. Effective leaching and extraction of valuable metals from electrode material of spent lithium-ion batteries using mixed organic acids leachant. *J. Ind. Eng. Chem.*, 79, 154–162. <https://doi.org/10.1016/j.jiec.2019.06.023>

- Gaines, L., 2018. Lithium-ion battery recycling processes: Research towards a sustainable course. *Sust. Mater. Technol.*, 17, e00068. <https://doi.org/10.1016/j.susmat.2018.e00068>
- Gao, W., Liu, C., Cao, H., Zheng, X., Lin, X., Wang, H., Zhang, Y. & Sun, Z., 2018. Comprehensive evaluation on effective leaching of critical metals from spent lithium-ion batteries. *Waste Manage.*, 75, 477–485. <https://doi.org/10.1016/j.wasman.2018.02.023>
- Hayrapetyan, S. S.; Mangasaryan, L. G. Tovmasyan, M. R. & Khachatryan, H. G., 2006. Precipitation of aluminum hydroxide from sodium aluminate, by treatment with formalin, and preparation of aluminum oxide. *Acta Chromatographica* 16, 192-203. <http://yadda.icm.edu.pl/yadda/element/bwmeta1.element.baztech-article-BAT3-0037-0020>
- Hietala, J., Vuori, A., Johnsson, P., Pollari, I., Reutemann, W. & Kieczka, H., 2016. Formic acid. In *Ullmann's Encyclopaedia of Industrial Chemistry*, Wiley-VCH Verlag GmbH & Co. KGaA, https://doi.org/10.1002/14356007.a12_013.pub3
- Ibiapina, V. F., Florentino, U. S., Afonso, J. C., Gante, V., Vianna, C. A. & Mantovano, J. L., 2018. Processing of spent zinc-MnO₂ dry cells in various acidic media. *Quim. Nova* 41, 176-183. <https://doi.org/10.21577/0100-4042.20170162>
- Janiszewska, M., Markiewicz, A. & Regel-Ros, M., 2019. Hydrometallurgical separation of Co(II) from Ni(II) from model and real waste solutions. *J. Cleaner Prod.*, 228, 746-754. <https://doi.org/10.1016/j.jclepro.2019.04.285>
- Josso, P., Roberts, S., Teagle, D. A. H., Pourret, O., Herrington, R. & Albaran, C. P. L., 2018. Extraction and separation of rare earth elements from hydrothermal metalliferous sediments. *Miner. Eng.*, 118, 106-121. <https://doi.org/10.1016/j.mineng.2017.12.014>
- Korkmaz, K., Alemrajabi, M., Rasmuson, Å. C. & Forsberg, K. M., 2018. Sustainable hydrometallurgical recovery of valuable elements from spent nickel-metal hydride HEV batteries. *Metals*, 8, 1062. <https://doi.org/10.3390/met8121062>
- Kulyakthin, S. & Pastye, A. K., 2021. Can calorimetry be used to measure the melting rate of deicers? *Cold Reg. Sci. Technol.*, 181, article 103170. <https://doi.org/10.1016/j.coldregions.2020.103170>
- Liu, X., Li, S., Liu, Y. & Cao, Y., 2015. Formic acid: A versatile renewable reagent for green and sustainable chemical synthesis. *Chinese J. Catal.*, 36, 1461–1475. [https://doi.org/10.1016/S1872-2067\(15\)60861-0](https://doi.org/10.1016/S1872-2067(15)60861-0)
- Lucas, J., Lucas, P., Le Mercier, T., Rollat, A. & Davenport, W., 2015. Rare earths in rechargeable batteries. *Rare Earths*, 167-180 (Chapter 10). <https://doi.org/10.1016/B978-0-444-62735-3.00010-3>
- Lurie, J., 1978. *Handbook of Analytical Chemistry*, 3rd ed. Mir, Moscow.
- Meshram, P., Pandey, B. D. & Mankhand, T. R., 2016. Process optimization and kinetics for leaching of rare earth metals from the spent Ni-metal hydride batteries. *Waste Manage.*, 51, 196-203. <https://doi.org/10.1016/j.wasman.2015.12.018>
- Meshram, P., Somani, H., Pandey, B. D., Mankhand, T. R., Deveci, H. & Abhilash, 2017. Two stage leaching process for selective metal extraction from spent nickel metal hydride batteries. *J. Cleaner Prod.*, 157, 322-332. <https://doi.org/10.1016/j.jclepro.2017.04.144>
- Meshram, P., Pandey, B. D. & Abhilash, 2019. Perspective of availability and sustainable recycling prospects of metals in rechargeable batteries – A resource overview. *Resour. Policy*, 60, 9-22. <https://doi.org/10.1016/j.resourpol.2018.11.015>
- Meshram, P., Mishra, & Sahu, R., 2020. Environmental impact of spent lithium ion batteries and green recycling perspectives by organic acids: a review. *Chemosphere*, 242, 125291. <https://doi.org/10.1016/j.chemosphere.2019.125291>
- Musariri, B., Akdogan, G., Dorfling, C. & Bradshaw, S., 2019. Evaluating organic acids as alternative leaching reagents for metal recovery from lithium ion batteries. *Miner. Eng.*, 137, 108-117. <https://doi.org/10.1016/j.mineng.2019.03.027>
- Oliveira, U. C. M., Rodrigues, G. D., Mageste, A. B. & Lemos, L. R., 2017. Green selective recovery of lanthanum from Ni-MH battery leachate using aqueous two-phase systems. *Chem. Eng. J.*, 322, 346–352. <https://doi.org/10.1016/j.cej.2017.04.044>
- Paulino, J. F., Neumann, R., Afonso, J. C., 2018. Production of sodium and aluminum chemicals and recovery of rare earth elements after leaching cryolite from Pitinga mine (Amazonas - Brazil) with sulfuric acid. *Hydrometallurgy*, 180, 254-261. <https://doi.org/10.1016/j.hydromet.2018.08.004>
- Reutmann, W., Kieczka, H., 2012. Formic Acid. *Ullmann's Encyclopedia of Industrial Chemistry*. Weinhein: Wiley-VCH Verlag, vol. 16, p. 13-33. https://onlinelibrary.wiley.com/doi/epdf/10.1002/14356007.a12_013.pub2
- Ritcey, G. M. & Ashbrook, A. W., 1984. *Principles and Applications to Process Metallurgy (Part I)*. New York, Elsevier Science Publishers.
- Shih, Y. J., Chien, S. K., Jhang, S. R. & Lin, Y. C., 2019. Chemical leaching, precipitation and solvent extraction for sequential separation of valuable metals in cathode material of spent lithium ion batteries. *J. Taiwan Inst. Chem. E.*, 100, 151–159. <https://doi.org/10.1016/j.jtice.2019.04.017>
- Santos, V. E. O., Celante, V. G., Lelisa, M. F. F. & Freitas, M. B. J. G., 2014. Método hidrometalúrgico para reciclagem de metais terras raras, cobalto, níquel, ferro e manganês de eletrodos negativos de baterias exauridas de Ni-MH de telefone celular. *Quim. Nova*, 37, 22-26. <http://dx.doi.org/10.1590/S0100-40422014000100005>
- Silva, R. G., Afonso, J. C. & Mahler, C. F., 2018. Acidic leaching of Li-ion batteries. *Quim. Nova*, 41, 581-586. <http://dx.doi.org/10.21577/0100-4042.20170207>
- Turek, A. S., 2018. Hydrometallurgical recovery of metals: Ce, La, Co, Fe, Mn, Ni and Zn from the stream of used Ni-MH cells. *Waste Manage.*, 77, 213-219. <https://doi.org/10.1016/j.wasman.2018.03.046>
- Valadares, A., Valadares, C. F., Lemos, L. R., Mageste, A. B. & Rodrigues, G. D., 2018. Separation of cobalt and nickel in leach solutions of spent nickel-metal hydride batteries using aqueous two-phase systems (ATPS). *Hydrometallurgy*, 181, 180-188. <https://doi.org/10.1016/j.hydromet.2018.09.006>
- van der Voorde, I., Pinoy, L., Courtijn, E., Verpoort, F., 2006. Equilibrium Studies of Nickel(II), Copper(II) and Cobalt(II) Extraction with Aloxime 800, D2EHPA, and Cyanex Reagents. *Solvent Extr. Ion Exc.*, 24, 893-914. <https://doi.org/10.1080/07366290600952717>
- Viirolainen, S., Ibane, D. & Paatero, E., 2011. Recovery of indium from indium-tin-oxide by solvent extraction. *Hydrometallurgy*, 107, 56-61. <https://doi.org/10.1016/j.hydromet.2011.01.005>
- Vogel, A. I., 1981. *Química Analítica Qualitativa*, 5ª ed. São Paulo: Mestre Jou.
- Wang, S., Wang, C., Lai, F., Yan, F. & Zhang, Z., 2020. Reduction-ammoniacal leaching to recycle lithium, cobalt, and nickel from spent lithium-ion batteries with a hydrothermal method: Effect of reductants and ammonium salts. *Waste Manage.*, 102, 122–130. <https://doi.org/10.1016/j.wasman.2019.10.017>
- Xie, F., Zhang, T.A., Dreisinger, D., Doyle, F., 2014. A critical review on solvent extraction of rare earths from aqueous solutions. *Miner. Eng.*, 56, 10-28. <https://doi.org/10.1016/j.mineng.2013.10.021>
- Yang, X., Zhang, J. & Fang, X., 2014. Rare earth element recycling from waste nickel metal hydride batteries. *J. Hazard. Mat.*, 279, 384–388. <https://doi.org/10.1016/j.jhazmat.2014.07.027>
- Yang, L., Yang, L., Xu, G., Feng, Q., Li, Y., Zhao, E., Ma, J., Fan, S. & Li, X., 2019. Separation and recovery of carbon powder in anodes from spent lithium-ion batteries to synthesize graphene. *Sci. Rep.*, 9, 9823. <https://doi.org/10.1038/s41598-019-46393-4>